

Tunable Polyaniline Chemical Actuators

Junbo Gao, José-María Sansiñena, and Hsing-Lin Wang*

Bioscience Division, Los Alamos National Laboratory, MSJ-586,
Los Alamos, New Mexico, 87545

Received November 13, 2002. Revised Manuscript Received April 2, 2003

Polyaniline (PANI) porous asymmetric membranes were prepared using a phase-inversion technique, and their bending–recovery behavior induced by sorption and desorption of chemical vapors was studied. It was found that the bending–recovery rates and maximum bending angles of the membranes were different in various vapors [hexane, ethyl ether, ethyl acetate, tetrahydrofuran (THF), and ethanol]. The undoped PANI membrane showed the most extensive and the fastest bending–recovery movement in THF but no bending–recovery movement in hexane. We believe that the bending–recovery movement results from the asymmetric structure of the membrane's cross section. The dense side has a larger volume expansion than the more porous side after the absorption of organic vapors, and this larger volume causes a bending toward the porous side. Desorption of organic vapor from the membrane allows it to recover to its original position. The study of the effect of the membrane structure on membrane bending–recovery behavior shows that changing the PANI emeraldine base (EB) concentration of the solution used to cast the PANI porous asymmetric membrane changes not only the mechanical properties of the membranes but also the bending–recovery rate of these membrane-based actuators. Lowering the EB concentration leads to the formation of a more porous structure, which increases the diffusion rate of the organic vapor into the membrane and thereby accelerates the bending–recovery movement induced by sorption and desorption. Reversing the hydrophobicity by doping PANI with the surfactant acid, dedecylbenzenesulfonic acid, allows the membrane to respond to less-polar organic vapors such as hexane. Simplified mechanisms between both doped and undoped PANI and organic vapors are proposed to explain the above results.

Introduction

Conducting polymer (CP) actuators have attracted considerable attention because of their lightweight, low operating potential, high mechanical strength, and potential applications in advanced robotics, microactuators, and artificial muscles.^{1–4} There are mainly two types of surrounding stimuli that can trigger the movement of CP actuators: electrical and chemical. Electrical potential can promote a movement in CP actuators because a volume change occurs during the electrochemical doping–dedoping process. In the past few years, most research efforts have focused on electrochemically driven CP actuators. Actuators with different configurations based on CP membranes or fibers have been fabricated that show either bending–recovery movement or linear extension.^{5–12} In addition, electro-

chemically triggered microactuators have recently been used to handle, transport, and separate biological species.¹³

Polymer actuators that can be chemically stimulated were discovered more than half a century ago when collagen filaments were demonstrated to reversibly contract or expand when dipped in acid or alkali aqueous solutions, respectively.¹⁴ This work prompted the development of synthetic polymers that mimic biological muscles.¹⁵ Chemically triggered actuators can isothermally transform chemical energy directly into mechanical work and are therefore called “mechanochemical” or “chemomechanical” actuators.^{16,17} Successfully fabricated chemomechanical rotors based on chemi-

* E-mail: hwang@lanl.gov.

(1) Baughman, R. H.; Schacklette, L. W. *Science and Applications of Conducting Polymers*; Adam Hilger: New York, 1990.

(2) Baughman, R. H.; Schacklette, L. W.; Elsenbaumer, R. L.; Plichta, E.; Becht, C. *Conjugated Polymeric Material: Opportunities in Electronics, Optoelectronics and Molecular electronics*; Kluwer: Dordrecht, The Netherlands, 1990; Vol. 559.

(3) Smela, E.; Ingnas, O.; Pei, Q. B.; Lundstrom, I. *Adv. Mater.* **1993**, *5*, 630–632.

(4) Baughman, R. H.; Schacklette, L. W.; Elsenbaumer, E.; Plichta, E.; Becht, C. *Microelectrochemical Actuators Based on Conducting Polymers*; Kluwer Academic Publishing: Dordrecht, The Netherlands, 1991; Vol. 267.

(5) Otero, T. F.; Rodriguez, J.; Angulo, E.; Santamaria, C. *Synth. Met.* **1993**, *57*, 3713–3717.

(6) Pei, Q. B.; Ingnas, O. *J. Phys. Chem.* **1992**, *96*, 10507–10514.

(7) Morita, S.; Shakuda, S.; Kawai, T.; Yoshino, K. *Synth. Met.* **1995**, *71*, 2231–2232.

(8) Pei, Q. B.; Ingnas, O. *Synth. Met.* **1993**, *57*, 3730–3735.

(9) DellaSanta, A.; DeRossi, D.; Mazzoldi, A. *Synth. Met.* **1997**, *90*, 93–100.

(10) Madden, J. D.; Cush, R. A.; Kanigan, T. S.; Brenan, C. J.; Hunter, I. W. *Synth. Met.* **1999**, *105*, 61–64.

(11) Mazzoldi, A.; DeglInnocenti, C.; Michelucci, M.; DeRossi, D. *Mater. Sci. Eng., C* **1998**, *6*, 65–72.

(12) Irvin, D. J.; Goods, S. H.; Whinnery, L. L. *Chem. Mater.* **2001**, *13*, 1143–1145.

(13) Jager, E. W. H.; Smela, E.; Ingnas, O. *Science* **2000**, *290*, 1540–1545.

(14) Katchalsky, A. *Experientia* **1949**, *5*, 319.

(15) Steinberg, I. Z.; Oplatka, A.; Katchalsky, A. *Nature* **1966**, *210*, 568.

(16) Kuhn, W.; Hargitay, B.; Katchalsky, A.; Eisenberg, H. *Nature* **1950**, *165*, 514.

cally triggered actuators show promise for use in transducing chemical free energy directly into mechanical work.^{18,19}

The fabrication of CP-engineered articles such as fibers and membranes has suffered from the fact that the fibers and membranes were neither soluble nor fusible. In many cases, CP thin films have been synthesized using electrochemical methods. Recent successes in the fabrication of polyaniline (PANI) membranes and fibers from highly concentrated PANI emeraldine base (EB) solution, as well as PANI's high environmental stability, low cost, facile redox potential, and relatively high conductivity, make it one of the most promising CPs for practical application in fabricating CP actuators.^{20–22} Previously, we reported the application, through doping and dedoping mechanisms, of PANI integrally skinned asymmetric membranes (PANI ISAMs) as monolithic chemical and electrochemical actuators in basic or acidic media.^{23,24}

In this study, we found that PANI porous asymmetric membranes undergo bending–recovery movement induced by sorption and desorption of organic vapor. This result is similar to that observed for electrochemically prepared polypyrrole chemical actuators in which polypyrrole films in the solid state undergo rapid and intensive bending–recovery movements. Bending–recovery movement in polypyrrole film was induced mainly by the reversible and anisotropic adsorption of aqueous vapor.^{18,19} Our PANI porous asymmetric membrane differs from the polypyrrole chemical actuators. First, the PANI membrane can be fabricated by a simple solution casting method, which is more efficient than the electrochemical method used to prepare other CP thin films. Second, the polypyrrole film bends upon asymmetrical exposure to stimuli; i.e., only one side of the film is exposed to the vapor. Our PANI porous asymmetric membrane bends upon homogeneous exposure to organic vapor. Third, and most important, the hydrophilicity or hydrophobicity of the PANI porous asymmetric membrane can be fine-tuned by doping the membrane with a surfactant acid, dodecylbenzenesulfonic acid (DBSA). Tuning PANI's hydrophobicity is very important for fabricating sensor arrays based on these PANI membranes. DBSA-doped membranes exhibit bending–recovery responses that are very different from those of undoped PANI membranes. In this paper, detailed mechanisms of the bending–recovery movement of PANI membranes are discussed and the effect of the membrane structure and different organic vapors on the bending–recovery rate and maximum bending angle are presented.

(17) Osada, Y. *Advances in Polymer Science*; Springer-Verlag: Berlin, 1987; Vol. 82.

(18) Okuzaki, H.; Kunugi, T. *J. Polym. Sci., Part B: Polym. Phys.* **1996**, *34*, 1747–1749.

(19) Okuzaki, H.; Kunugi, T. *J. Appl. Polym. Sci.* **1997**, *64*, 383–388.

(20) Wang, H. L.; Romero, R. J.; Mattes, B. R.; Zhu, Y. T.; Winokur, M. J. *J. Polym. Sci., Part B: Polym. Phys.* **2000**, *38*, 194–204.

(21) Mattes, B. R.; Wang, H. L.; Yang, D.; Zhu, Y. T.; Blumenthal, W. R.; Hundley, M. F. *Synth. Met.* **1997**, *84*, 45–49.

(22) Mattes, B. R.; Wang, H. L. U.S. Patent 5,981,695, Nov 9, 1999.

(23) Wang, H. L.; Mattes, B. R. *Synth. Met.* **1999**, *102*, 1333–1334.

(24) Wang, H. L.; Gao, J. B.; Sansinena, J. M.; McCarthy, P. *Chem. Mater.* **2002**, *14*, 2546–2552.

Experimental Section

Materials. 1-Methyl-2-pyrrolidinone (NMP), heptamethylenimine (HPMI), tetrahydrofuran (THF), hexane, diethyl ether, ethyl acetate, methanol, ethanol, and DBSA (70 wt % solution in 2-propanol) were purchased from Aldrich and used without further purification. PANI EB powder was purchased from Neste Oy and was used as received.

Preparation of PANI Membrane Using Water as the Coagulation Bath. In a typical procedure, 3.70 g of NMP (from Aldrich, dried by a 4 Å molecular sieve) was put into a 12.0 mL Teflon vial. Then 0.31 g of HPMI (from Aldrich) was added to it. The vial was sealed with a Teflon cap and kept in an oven at 60 °C for 5 min. Then 1.00 g of EB powder was added to the vial. The solution was stirred slowly with a homogenizer and then ramped up to 5000 rpm for 25 min. The EB/HPMI molar ratio was 1:1 (the moles of EB are calculated based on the tetrameric repeat unit). The resulting EB solution was poured onto a glass plate and spread into a wet film using a gardener's blade with a preset thickness (Pompano Beach, FL). The wet film was then immersed into the water bath and kept in the water bath for more than 24 h. The film was then dried under vacuum at room temperature for 12 h before measuring the mechanical properties and evaluating its performance as a chemical sensor/actuator. Using the same procedure, we prepared membranes from EB solutions with concentrations of 17.5, 20, and 22.5 wt %.

Morphology Characterization. Cross sections of the PANI porous asymmetric membranes were prepared by breaking the membrane samples in liquid nitrogen. Membrane freeze-fracturing kept the cross-sectional structure of the membrane intact. The surface of the membrane was coated with a thin layer of carbon prior to taking scanning electron microscopy (SEM) measurements.

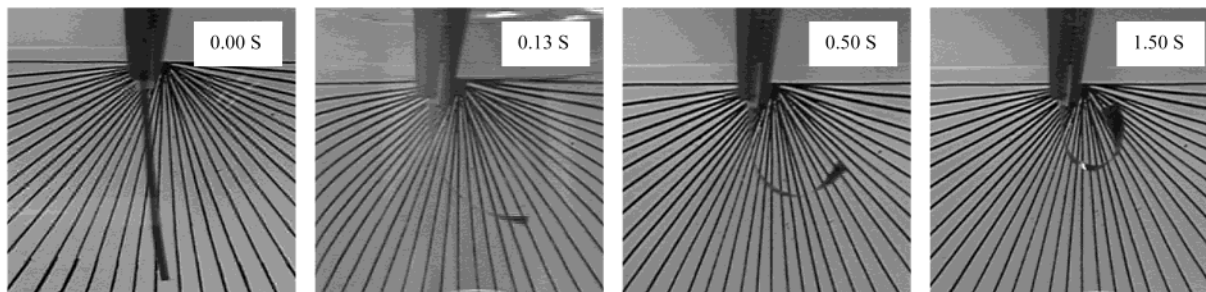
Mechanical Test Measurement. Mechanical properties of the membranes were measured using a Shimadzu EZ-TEST instrument controlled by a Pentium III Dell computer using the WinAGS Lite software. All of the measurements were performed using a strip 40.0 mm in length and 2.0 mm in width cut from an as-prepared PANI membrane. Both ends of the strip were held by the grips of the instrument, one by the top grip and the other one by the bottom grip. The membrane was stretched at a controlled, constant speed of 1 mm/min, and the curve of stress versus strain was obtained.

Chemical Actuator Measurement. The chemical actuators were constructed using strips 40.0 mm long and 2.0 mm wide cut from the PANI membrane. The strips were fixed at one end, leaving the other end free to move. The strip was exposed to hexane, diethyl ether, ethyl acetate, THF, and ethanol vapors at room temperature, and the bending–recovery movement was characterized. After the free end of the membrane reached a maximum angle, it was removed from the organic vapor, and the free end recovered to its original position. To better control the experimental conditions, the organic vapors were prepared by putting 10 mL of the solvent into a 200 mL beaker. The beaker was sealed with a plastic film with a small hole in it, and the membrane was inserted into the beaker through this hole. A simple, homemade device, in which an angular plot was placed behind the actuator, was used to monitor the bending angle. The bending–recovery movements of the membrane in organic vapor and in air are shown in Figure 1. The geometrical changes of the strip were recorded using a Panasonic digital video camcorder. The bending angle of the strip was calculated by the degree of movement at the free end. The experiments were repeated three times, and an experimental error of 5% was calculated.

Results and Discussion

Chemomechanical Behavior of the PANI Porous Asymmetric Membrane in Organic Vapors. A series of pictures demonstrating the bending–recovery movement at different time scales of a PANI porous asymmetric membrane exposed to THF vapors is shown in

In THF Vapor



In Air

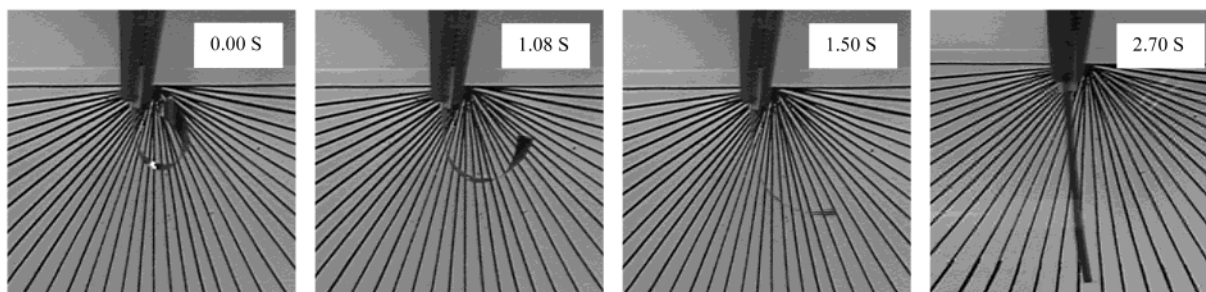


Figure 1. Bending–recovery movement of a chemical vapor triggered actuator in organic vapor and in air.

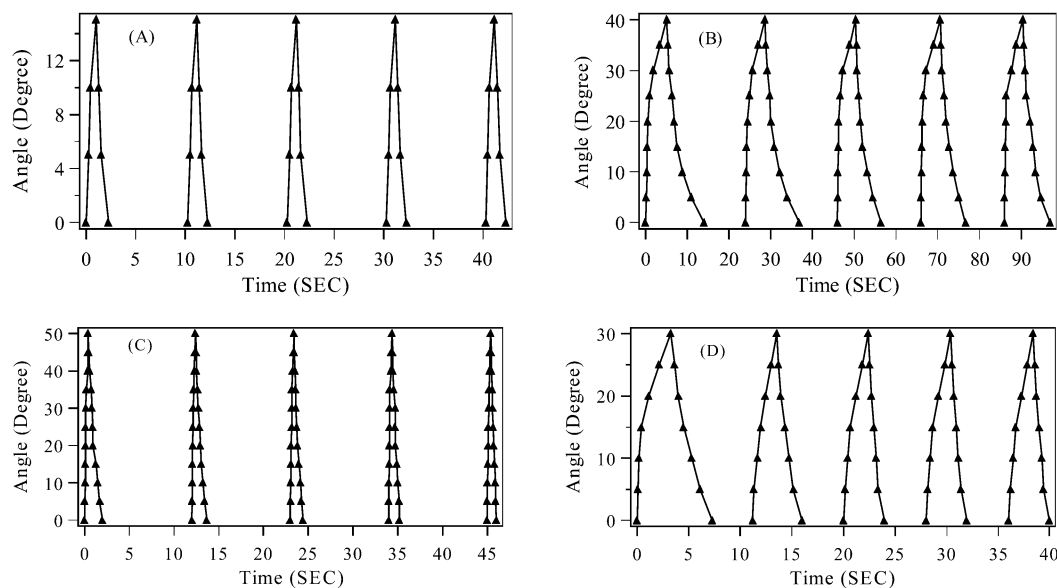


Figure 2. Bending–recovery movement of PANI porous asymmetric membranes in different saturated organic vapors: (A) diethyl ether; (B) ethyl acetate; (C) THF; (D) ethanol.

Figure 1. In this figure, we can clearly see that the PANI membrane bends more than 90° in 1.5 s and takes 2.7 s to recover to its original position. Based on these pictures, we can plot the time profile of the bending–recovery angle for the PANI porous asymmetric membrane cast from a 20.0 wt % EB solution in different organic vapors (see Figure 2). In all of these experiments, the PANI porous asymmetric membrane bent once it was exposed to the organic vapor and then recovered to its original position when it was removed from the organic vapor. Figure 2 also shows that the PANI porous asymmetric membrane has different maximum bending angles and bending–recovery rates in different organic vapors. For example, the membrane

does not show any movement in hexane, and the bending angle increases gradually as it is exposed to diethyl ether, ethanol, ethyl acetate, and THF.

It should be noted that the bending–recovery behavior of the PANI membrane in THF vapor is somewhat different from its behavior when exposed to the rest of the vapors. In THF vapor, the membrane bends continuously to form a loose spiral. In other vapors, the membrane bends and stops at a maximum angle, typically $<70^\circ$. Removal of the membrane from THF vapor leads the loose spiral to recover to its original shape almost immediately. To better compare the bending–recovery rates and angles, the membranes were only allowed to bend to 50° in THF and then transferred

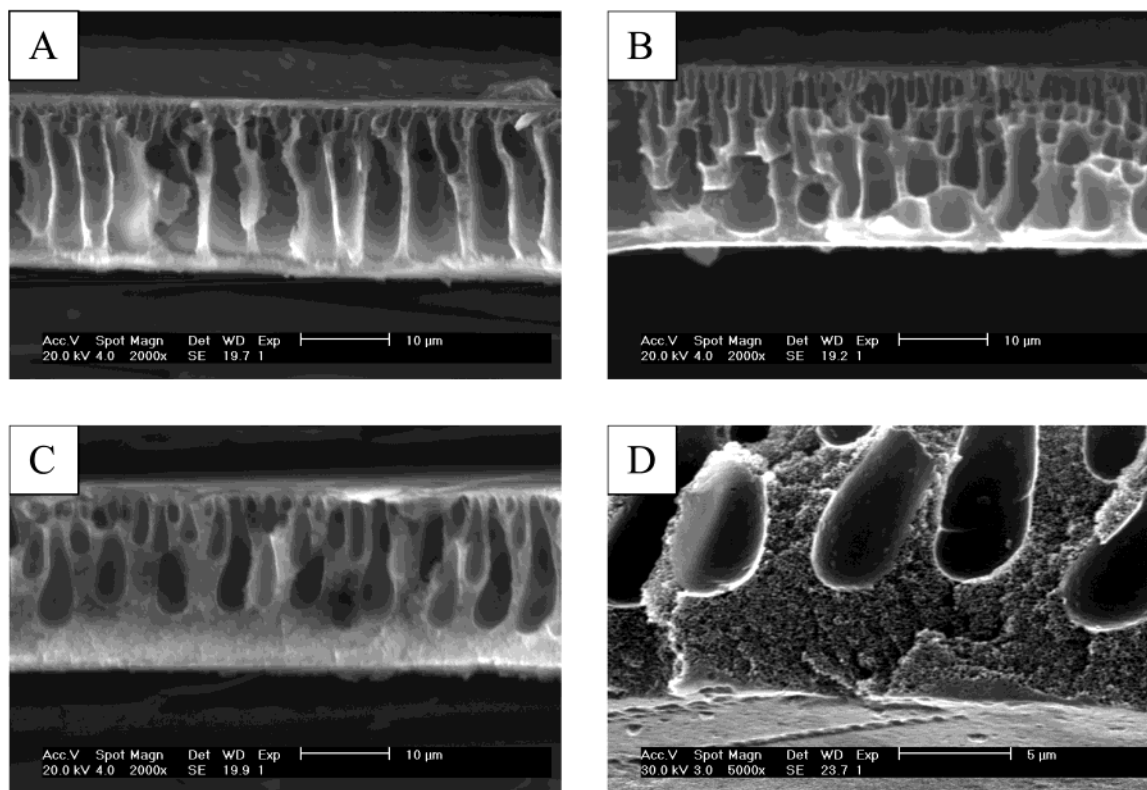


Figure 3. SEMs of the cross sections of membranes cast from different solutions: (A) 17.5 wt % EB solution; (B) 20.0 wt % EB solution; (C) 22.5 wt % EB solution; and (D) magnification of part C.

to air for recovery. In addition to the differences in maximum bending angles, PANI porous asymmetric membranes show big differences in bending–recovery rates in different vapors. The bending–recovery rate in hexane is 0 and increases in ethyl acetate, ethanol, diethyl ether, and THF. Among all of the organic vapors, THF causes the fastest bending–recovery movement and most extensive bending angle.

Bending–recovery movement of PANI porous asymmetric membranes in organic vapors was found to be highly thickness-dependent. The bending angle and bending–recovery rate of the membrane in organic vapors decrease sharply with an increase in the membrane thickness. For example, a 25 μm PANI porous asymmetric membrane cast from a 20.0 wt % EB solution has a fast bending–recovery movement in THF. It can finish a bending–recovery cycle (with a 50° maximum bending angle) within 2 s. However, it takes a 40 μm membrane cast from the same solution 5 s to bend to 50° when exposed to THF vapor and 6 s to recover to its original position. Therefore, it takes a total of 11 s to finish a bending–recovery cycle (figure not shown here). This result suggests that the bending–recovery movement is determined by a diffusion-dominated mechanism. Although a thinner membrane is always superior to a thicker one in terms of the bending–recovery rate, further reducing the thickness leads to a structural defect, and the porous asymmetric membrane becomes very brittle. Using a phase-inversion technique, a membrane with a thickness of ~25 μm is the thinnest free-standing membrane we can make.

Bending–Recovery Mechanism of the Membrane in Organic Vapors. Parts A–C of Figure 3 exhibit typical cross-sectional structures of PANI porous

asymmetric membranes prepared using a phase-inversion technique. The top side of Figure 3B corresponds to the side of the wet film in direct contact with the air, and the bottom side corresponds to the side of the film in contact with the glass substrate. It is clear that the size of the macrovoids increases gradually from the denser side (top side) to the porous side (bottom side) along the cross section of the membrane. This decrease in macrovoid size across the membrane leads to an asymmetrical configuration.

In the experimental procedure to fabricate PANI membranes, NMP was used as the solvent and a small amount of hexamethylenimine was used as the gel inhibitor.²² The small amount of gel inhibitor plays a key role in the formation of a highly concentrated, homogeneous EB solution because it prevents the formation of intrachain and interchain hydrogen bonds.^{21,22} Because of the high affinity between NMP and water, an instantaneous solvent–nonsolvent exchange occurs when the EB solution is immersed in a water bath, and an asymmetric porous asymmetric membrane is formed.

Previously, we found that the asymmetric PANI membrane can bend in an acidic solution and recover in a basic solution.²⁴ This bending–recovery movement results from the chemical doping–dedoping process. Doping leads to incorporation of the dopants within the backbone of PANI chains, which causes the bulk volume to increase. Because of the asymmetric structure of the membrane's cross section, a density-dependent volume expansion creates a stress gradient and promotes the bending–recovery movement of the membrane.²⁴ However, the bending–recovery movements of PANI porous asymmetric membranes studied in this work were caused only by the physical sorption and desorption of

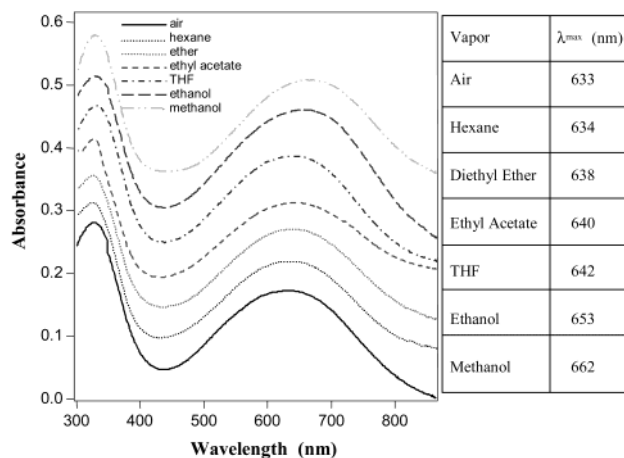


Figure 4. UV-vis spectra of PANI membranes in air and in various organic vapors.

organic vapor and involved no chemical reaction. The volumetric change of the membrane can be explained in terms of a conformational change in the PANI chains due to the sorption and desorption of organic vapor. After the sorption of organic vapor, the PANI chains in the membrane extend, which causes the volume to expand.

Because of the asymmetric structure of the membrane, a density-dependent volume expansion is created along the cross section and makes the membrane bend as it is exposed to organic vapors. When the membrane is removed from the organic vapor and placed in air, the desorption of the vapor in the membrane causes the volume to contract to its original value, and a stress gradient in the opposite direction is generated that causes the membrane to recover to its original position.

Figure 4 shows the UV-vis spectra of a PANI thin film measured in air and in different organic vapors. There are two peaks in the UV-vis spectra of the EB film. The peak at 330 nm is due to the $\pi-\pi^*$ transition, and the peak at 633 nm corresponds to the exciton transition. This exciton peak is generated by the electron transition from a benzene ring to a quinoid ring along the PANI chain. From Figure 4, one can see that EB chain extension upon exposure to chemical vapor is manifested in the UV-vis spectra. The exciton peak position shifts to 634, 638, 640, 642, 653, and 662 nm after exposure to hexane, diethyl ether, ethyl acetate, THF, ethanol, and methanol vapors, respectively. It is known that the red shift of the exciton peak can be induced by an increase in the effective conjugation length, which is caused by the extension of the polymer chain upon exposure to organic vapors.²⁵⁻²⁷ Because of the hydrophilic nature of PANI chains, the higher the polarity of the organic vapor, the larger the interaction with polymer chains will be. Our results show consistency with the above hypothesis, taking into account the polarity of the organic vapors studied (hexane < diethyl ether < ethyl acetate < THF < ethanol < methanol).

However, these results do not completely agree with the maximum angle shown in Figure 2 because one may expect that the larger the red shift (stronger interaction

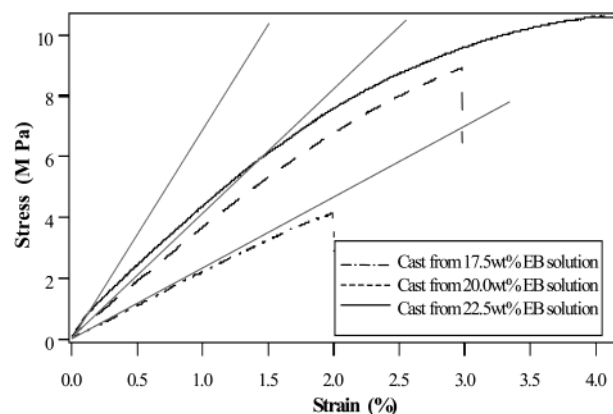


Figure 5. Stress-strain curves of membranes cast from different EB concentration solutions.

with polymer chains), the larger the maximum bending angle will be. This inconsistency in the red shifts of UV-vis spectra and maximum bending angles may be due to the number and sizes of the absorbed molecules that can affect the maximum angle in all cases. Therefore, the stronger affinity between polymer chains and organic vapor does not necessarily lead to greater bending angles.

Effect of the EB Concentration on the Structure, Mechanical Properties, and Bending-Recovery Rate of the Membrane. Parts A-C of Figure 3 show SEMs of the cross sections of PANI membranes cast from 17.5, 20.0, and 22.5 wt % EB solutions, respectively. The SEMs show that both the number and the size of the macrovoids decrease as the EB concentration of the solution used to prepare the membrane increases from 17.5 to 22.5 wt %. The higher polymer concentration seems to suppress the formation of macrovoids. Macrovoid formation is typically caused by instantaneous demixing between solvents and nonsolvents with high affinity such as NMP and water.²⁸ A lower polymer concentration solution takes a longer time to form a dense layer at the air-solution interface. This dense layer has no microporous judging from SEM. Increasing the polymer concentration results in a shorter time duration to form a dense skin. Skin formation leads to a slower flux rate for the nonsolvent (water) and results in the formation of a cellular structure with fewer macrovoids.²⁹

The mechanical strength (Young's modulus, determined by the slope of the tangent line of the stress-strain curve) directly correlates with the maximum work force that these membranes can generate once converted into actuators. Therefore, the mechanical properties of the PANI porous asymmetric membranes were measured. The stress-strain curves for the membranes are shown in Figure 5. From this figure, one can see that the Young's modulus and the break strain of the membrane increase with increases in the EB concentration that was used to fabricate the membranes. The membranes cast from 17.5, 20.0, and 22.5 wt % solutions show 218, 370, and 476 MPa Young's

(25) Zheng, W.; Min, Y.; MacDiarmid, A. G.; Angelopoulos, M.; Liao, Y. H.; Epstein, A. J. *Synth. Met.* **1997**, *84*, 63-64.

(26) Dimitriev, O. P. *Synth. Met.* **2001**, *125*, 359-363.

(27) Ghosh, S. Y. *Chem. Phys. Lett.* **1994**, *226*, 344-348.

(28) Mulder, M. *Basic Principles of Membrane Technology*, 2nd ed.; Kluwer Academic: Dordrecht, The Netherlands, 1991.

(29) Kim, Y. D.; Kim, J. Y.; Lee, H. K.; Kim, S. C. *J. Appl. Polym. Sci.* **1999**, *74*, 2124-2132.

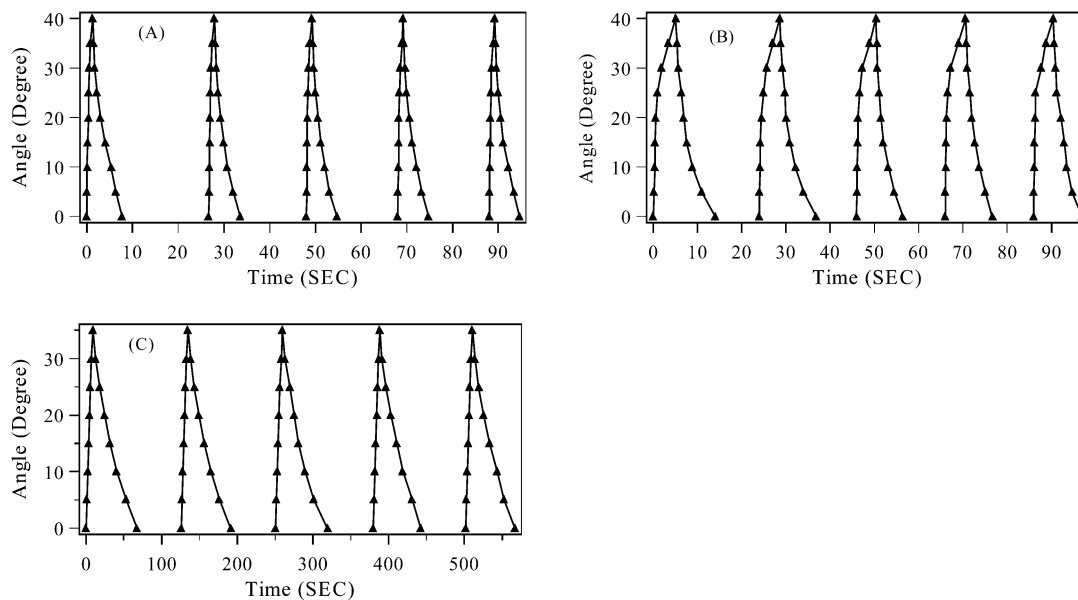


Figure 6. Bending–recovery movements of PANI porous asymmetric membranes cast from different EB concentration solutions in saturated ethyl acetate vapor: (A) 17.5 wt % EB solution; (B) 20.0 wt % EB solution; (C) 22.5 wt % EB solution.

moduli and 2.06%, 2.96%, and 4.12% break strain, respectively.

The fact that the membrane cast from the higher-concentration solution is stronger than the one cast from the lower-concentration solution can be explained by the cross-sectional structure of the membranes (see Figure 3A–C). By comparing the size and number of the macrovoids, one can see that a higher EB concentration can lead to the formation of membranes with higher EB mass content. This is further proven by the density measurements performed in which the membranes cast from 17.5, 20.0, and 22.5 wt % show a density of 0.289, 0.349, and 0.412 g/cm³, respectively. The membranes with higher polymer mass content certainly have a higher Young's modulus. They also have a larger break strain because the macrovoids can lead to defects during the stretching process.

Parts A–C of Figure 6 show the time profiles for bending–recovery in membranes of the same size (40 mm long, 20 mm wide, and approximately 25 μ m thick) cast from different solution concentrations (17.5, 20.0, and 22.5 wt %) in response to the same vapor (ethyl acetate vapor). This figure shows that the bending–recovery rates decrease with decreases in the concentration of the solution used to cast the membrane. Membranes cast from 17.5, 20.0, and 22.5 wt % concentrations took approximately 7.0, 12.8, and 65.0 s, respectively, to finish a bending–recovery cycle.

The bending–recovery movement of the membrane is controlled by the sorption and desorption of organic vapor. These results for the bending–recovery rates of membranes prepared from various EB concentrations show that sorption and desorption of organic vapor in the membrane cast from solution with lower EB concentrations are much faster than those in the membrane prepared from solution with higher EB concentrations. Moreover, compared to the membranes cast from 17.5 and 20.0 wt % EB solutions, the maximum bending angle of the membrane cast from 22.5 wt % is 5° smaller. This decrease in the bending angle can be explained by the cross-sectional structure of the membrane. As shown

in Figure 3A, the macrovoids expand across the membrane cast from a 17.5 wt % EB solution. This expansion makes the sorption and desorption of the vapor in the membrane very easy. The formation of smaller-size macrovoids in the membrane cast from 20.0 wt % blocks the sorption and desorption of organic vapor and therefore leads to a slower bending–recovery movement. In the membrane cast from a 22.5 wt % EB solution, the macrovoids become even smaller, and a microvoid structure is formed in the porous side (Figure 3D), which makes the sorption and desorption of the vapor even more difficult. Because the cross-sectional structure has a significant effect on the bending–recovery behavior of the membrane, the maximum bending angle and bending–recovery rate can be fine-tuned by using membranes cast from solutions with different concentrations.

Reversal of Hydrophilicity of PANI Membrane and Its Response to Organic Vapor. The membrane cast from a 20.0 wt % EB solution was doped in a 10.0 wt % DBSA/water/2-propanol (20 v/v) solution for 12 h and subsequently dried under vacuum at room temperature for 48 h. The conductivity of the doped membrane is \sim 0.1 S/cm, which suggests that this membrane is fully doped. A 40 \times 2 mm piece was cut from the DBSA-doped membrane, and the bending–recovery movement was measured by the method mentioned in the preceding section. To prevent disturbance from other vapors, a fresh membrane was used in each experiment. The results for the bending–recovery rate of the PANI porous asymmetric membrane doped by DBSA are shown in Figure 7B. Comparing the bending–recovery rates of the undoped PANI membranes (Figure 7A) and DBSA-doped membranes, we see the following differences: (1) Undoped EB membranes show no movement in hexane, and DBSA-doped membranes show a 25° reversible bending–recovery movement. (2) EB membranes show the most extensive bending angle and the fastest bending–recovery movement in THF, and DBSA-doped membranes shows the most extensive bending angle and fastest bending–recovery movement in di-

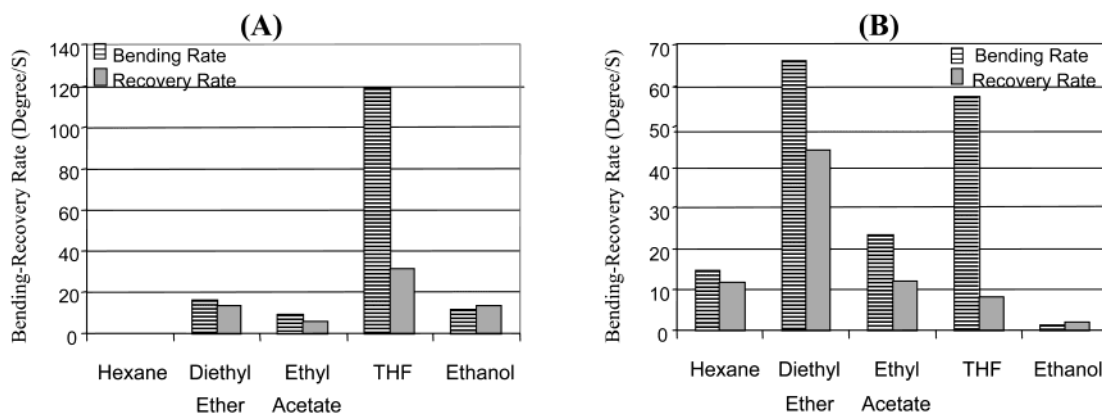


Figure 7. Bending–recovery rate of undoped and DBSA-doped PANI membranes in different organic vapors: (A) undoped PANI membrane; (B) DBSA-doped PANI membrane.

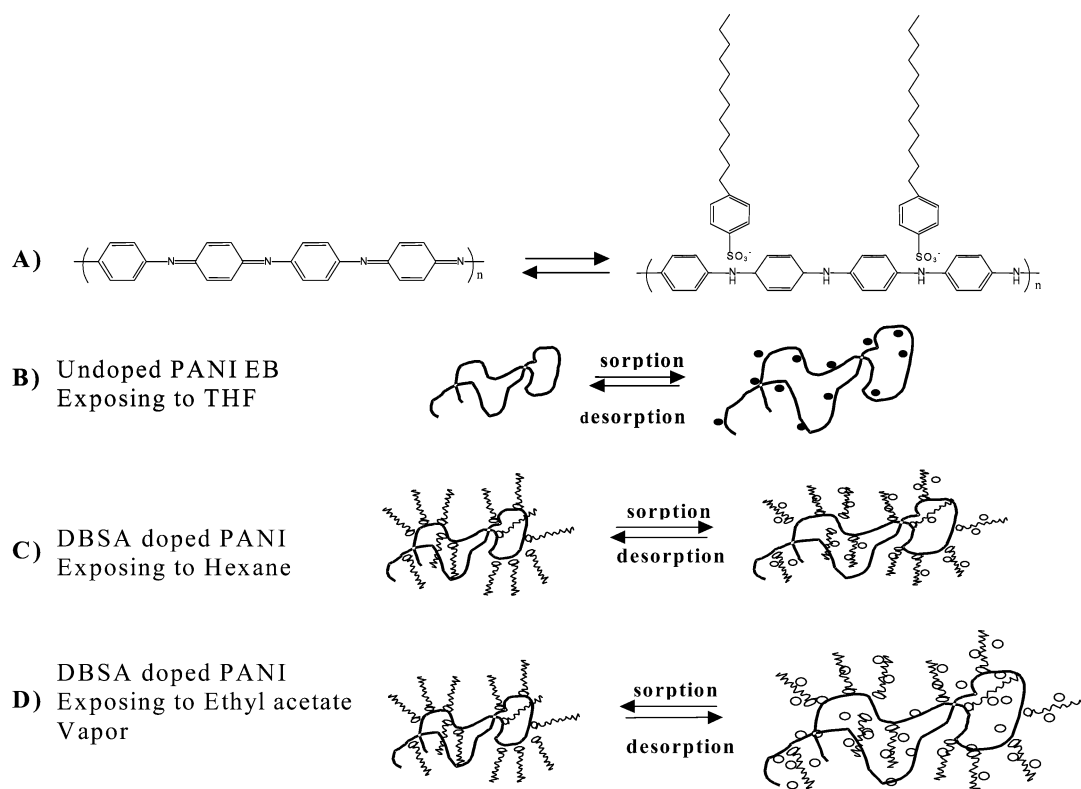


Figure 8. (A) Molecular structure of undoped PANI and DBSA-doped PANI. (B) Sorption and desorption of THF in undoped PANI. (C) Sorption and desorption of hexane in DBSA-doped PANI. (D) Sorption and desorption of ethyl acetate in DBSA-doped PANI.

ethyl ether vapor. (3) After doping by DBSA, the bending–recovery rate increases in hexane, diethyl ether, and ethyl acetate vapor and decreases in THF and ethanol vapor.

As mentioned above, the bending–recovery movement of the PANI porous asymmetric membranes is mainly determined by the kinetics of sorption and desorption of organic vapors. The bending–recovery movement is therefore highly dependent on the affinity between the PANI chain and the organic vapors. DBSA-doped PANI has the carboxylate groups complex with the PANI backbone and the hydrophobic aliphatic tails point outward, therefore turning the PANI membrane partly hydrophobic (see Figure 8). The contact angle measurements (the smaller the contact angle, the higher the hydrophilicity) for DBSA-doped PANI (74°) and undoped PANI (44°) substantiate the above hypothesis and

corroborate that DBSA doping changes the hydrophilicity of the PANI membrane and further alters the interaction between the PANI membrane and the organic vapors. On the one hand, the interaction between DBSA-doped PANI and less-polar vapors (such as hexane, diethyl ether, and ethyl acetate) is stronger than the interaction between the undoped PANI and the same vapors. On the other hand, the interaction between DBSA-doped PANI with polar vapors (such as THF and ethanol) is weaker than the interaction between the undoped PANI and the same vapors.

The differences in interaction between DBSA-doped and undoped membranes and more- and less-polar vapors affect the kinetics of the sorption and desorption of various organic vapors as well as the bending–recovery rate of the PANI membranes. For the less-polar vapors (hexane, diethyl ether, and ethyl acetate), the

bending–recovery rate of DBSA-doped PANI membrane increases. For the more-polar vapors (THF and ethanol), the bending–recovery rate decreases. We try to explain these results as follows (see also Figure 8): The undoped PANI membranes show no response to hexane vapor because the PANI chain does not absorb the less-polar vapor due to the weak interaction. However, the DBSA-doped PANI membrane responds to hexane vapor favorably because of the stronger interaction between the aliphatic tails of DBSA and the hexane molecules (Figure 8B). Diethyl ether and ethyl acetate vapors solvate both the PANI chain and the aliphatic tails of DBSA; therefore, the bending–recovery rate of the DBSA-doped PANI membrane increases (Figure 8C). THF and ethanol (polar vapors) can solvate only the PANI chain, and the aliphatic tails of DBSA slightly hinder the absorption of these polar vapors; therefore, the bending–recovery rate decreases.

Conclusion

PANI porous asymmetric membranes were prepared and subsequently used as chemical actuators. The membranes showed bending–recovery movement when exposed to organic vapors and recovered after removal from organic vapors. This bending–recovery movement is caused by the sorption and desorption of organic vapors. After the sorption of organic vapors, PANI chains expand to form an extended conformation, and the expansion increases the volume of the membrane.

After desorption of organic vapors, the PANI chains recover to a compact conformation, and the volume of the membrane changes to its original value. Because of the asymmetrical structure along the cross section of the membrane, the volume change caused by the sorption and desorption of organic vapor prompts a bending–recovery movement.

The maximum bending angles and bending–recovery rates of PANI porous asymmetric membranes are polarity- and density-dependent. The kinetics of organic vapor sorption and desorption are determined by the interaction between PANI chains and the vapor molecules. DBSA-doped PANI membranes become hydrophobic and therefore respond favorably to the less-polar vapors. The fact that the bending–recovery movement of PANI porous asymmetric membranes in response to the sorption and desorption of organic vapors is polarity-dependent and can be fine-tuned by changing the membrane's hydrophilicity makes PANI a suitable material from which to develop chemical sensors and actuators.

Acknowledgment. We thank the Cross Enterprise Technology Development Program of the National Aeronautics and Space Administration and the Laboratory Directed Research and Development fund of Los Alamos National Laboratory, a U.S. Department of Energy Laboratory, for their financial support of this project.

CM020329E